Cavitation 91 Symposium, 1st ASME-JSME Fluids Engineering Conference , 23-27 June 1991, Portland (Oregon)

CAVITATION EROSION POWER

F. Avellan, Ph. Dupont, M. Farhat
IMHEF-Institut de Machines Hydrauliques et de Mécanique des Fluides
EPFL- Swiss Federal Institute of Technology, Lausanne,
Switzerland

ABSTRACT

With a view to a proper setting of hydraulic machines a hydrodynamic definition of the cavitation "intensity" is introduced independently of the blade material property. This definition is based on the observation that as far as severe erosion is concerned we may consider a corresponding development of a leading edge cavity on the blades of the runner. Blade erosion is due to the collapse of transient swirling cavities in the closure region of the main cavity. According to the generation process of these transient cavities a mean erosive power of the cavities is evaluated from the upstream velocity U_∞, the main cavity length l and the Strouhal number S of the fluctuation of the cavity. This definition leads to a term proportional to $S\, U_\infty^3 l^2$. The experimental data obtained from erosion, vibration and shock overpressure measurements tends to collapse to a single curve. However, these results make it possible to establish a procedure for predicting the erosion risk of the prototype units by using cavitation tests on the model.

NOMENCLATURE

H	Net head		[m]
NPSH	Net positive suction head		[m]
n	Runner speed		[min^{-1}]
Q	Flow rate		[$m^3 \cdot s^{-1}$]
R	Turbine runner outlet radius or pump impeller inlet radius		[m]
n_q	Specific speed of the machine	$\frac{n\, Q_2^{\frac{1}{2}}}{H_4^{\frac{3}{4}}}$	[min^{-1}]
ω	Runner angular velocity		[s^{-1}]
φ	Flow coefficient	$\frac{Q}{\pi \omega R^3}$	[-]
ψ	Head coefficient	$\frac{2gH}{\omega^2 R^2}$	[-]
ν	Specific speed of the machine	$\frac{\varphi_2^{\frac{1}{2}}}{\psi_4^{\frac{3}{4}}}$	[-]
η	Machine efficiency		[-]
σ	Thoma's cavitation number	$\frac{NPSH}{H}$	[-]
E	Maximum potential energy of a transient cavity		[J]
$\dot{E}$	Cavitation erosion power		[W]
f	Pulsation frequency of the leading edge cavity		[Hz]
l	Cavity length		[m]
p_{max}	Maximum value of the static pressure in the closure region of a leading edge cavity		[Pa]
p_{ref}	Static pressure in the downstream vessel (CVG)		[Pa]
p_v	Vapor pressure		[Pa]
p_{wall}	Wall static pressure (CVG)		[Pa]
p_∞	Upstream pressure (cavitation tunnel)		[Pa]
U	Mean axial velocity in the inlet pipe (CVG)		[$m \cdot s^{-1}$]
U_∞	Upstream velocity (cavitation tunnel)		[Pa]
V	Maximum volume of a transient cavity		[m^3]
σ	Cavitation number (cavitation tunnel)	$\frac{p_\infty - p_v}{\frac{1}{2}\rho U_\infty^2}$	[-]
σ	Cavitation number (CVG)	$\frac{p_{ref} - p_v}{\frac{1}{2}\rho U^2}$	[-]
g	Gravity acceleration		[ms^{-2}]
ρ	Water density		[$kg \cdot m^{-3}$]
C_{pwall}	Wall pressure coefficient (CVG)	$\frac{p_{wall} - p_v}{\frac{1}{2}\rho U^2}$	[-]
S	Strouhal number	$\frac{f \cdot l}{U_\infty}$	[-]

INTRODUCTION

In the field of hydraulic machines, cavitation erosion is one of the main limiting features in the modern trend towards designing hydraulic machines with higher specific power and better reliability. For a given operating range, cavitation development is obviously influenced by the flow incidence angles, the hydrodynamic design of the runner and the setting level. 3-D flow computation allows us to predict the flow angles at the runner inlet, and the use of an inverse method of hydraulic runner design leads to an optimization of the shape of the blades. Thus, the setting level becomes the single remaining parameter which allows the cavitation development in a modern hydraulic machine to be controlled in order to avoid cavitation erosion.

Accurate determination of the setting level is very important in relation to high unit capacity and civil engineering costs. Usually the so-called cavitation tests are conducted on model machines, [1], and the NPSH influence on the performance characteristics of the pump, or of the turbine, are traced. One of these tests on a pump model, $n_q = 38$, is shown in Figure 1, where η - σ curves, the efficiency

versus cavitation number, are given for different operating points. A fall-off in efficiency can be used to define various levels such as σ_o, related to the beginning of the efficiency drop, or $\sigma_{3\%}$ corresponding to a 3% efficiency drop. In the first instance, a plant NPSH is selected in order to avoid cavitation erosion with an adequate safety margin referred to these levels σ_o or $\sigma_{3\%}$, regardless of the type of cavitation involved in the actual tests (Figure 2). This simple practice of referring to a hydraulic performance criterion, say $\sigma_{3\%}$, can be used successfully for small pumps, but the method is unsuccessful for large high-head units, in both pumps and turbines. For large units the setting must be improved through cavitation observation during model tests.

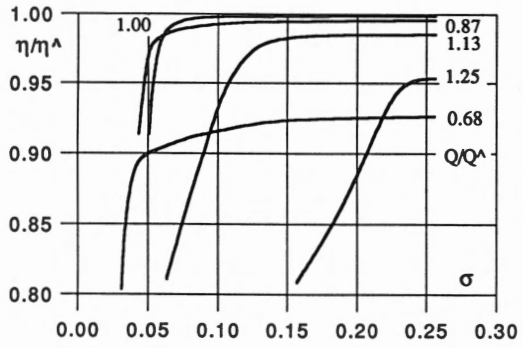

Fig. 1. Storage pump efficiency η as a function of the cavitation number σ for different operating points. The efficiency η and the flow rate Q are normalized by their value at the best efficiency operating point, η_Λ and Q_Λ respectively.

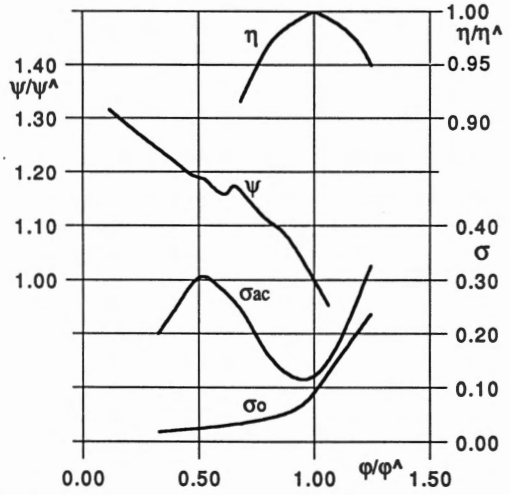

Fig. 2. $n_q = 38$ storage pump characteristics at constant speed with both σ_o and acceptable (σ_{ac}) evolution with the flow coefficient φ_1 at the impeller eye. All coefficients are related to their value at the best operating point quoted with ^.

In this case, it is current practice to define empirically an acceptable cavity length (Figure 3) as a reference for the setting determination, but this length obviously depends on the nominal head of the actual machines. Furthermore, the resulting setting level is very sensitive to the cavity length when the cavity is visible on the suction side. For instance, a typical cavity length evolution, versus the cavitation number σ, is given in Figure 4. The reported values were obtained during a cavitation test on an $n_q = 45$ storage pump model on the IMHEF Universal Hydraulic Machine Test Rig. All the model design requirements necessary for acceptance tests were fulfilled, in particular a rigorous geometrical homology with the prototype, and large windows installed at the inlet cone. Even under these best experimental test conditions, it was difficult to measure this length with an accuracy better than 1 mm on the blade. By taking into account this uncertainty on the curve of Figure 4 for the value of 10 mm, which corresponds to an acceptable cavity length value, the corresponding σ value is 0.182 within a range of $\pm$ 0.006. Since in this case the nominal head of the prototype was 250 m, the setting level could be estimated at 45.5 m to within $\pm$ 1.5 m. It should be emphasized that this uncertainty is due only to lack of accurate observation, without taking into account the arbitrary character of the acceptable length definition. Moreover, for a high discharge operating point, in the case of centrifugal pumps, the cavity which extends on the blade pressure side is not visible.

Fig. 3. Leading edge cavitation on an $n_q = 45$ storage pump model; $Q/Q_\Lambda = 0.9$ and $\sigma = 0.147$. White lines on the blade suction side are traced every 10 mm from the leading edge.

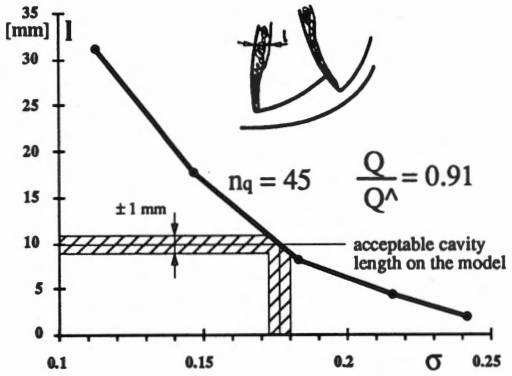

Fig. 4. Leading edge cavity length evolution l with the cavitation number σ for the same storage pump model as in Figure 3.

To overcome these empirical approaches for the determination of the setting level, an erosion test could be performed with the actual model by using paint or soft material. These tests have been carried out and analyzed by many researchers see for instance [2], [3]. But the need to use the material damage itself as a measure of the cavitation erosiveness adds to a rather difficult hydrodynamic problem another one concerning the transposition of a soft material behavior to the one of the actual material of interest. However the transposition of the results to the prototype scale is not very accurate and does not lead to a better confidence in the NPSH determination,

despite the extraneous testing costs. A new approach based on the similarity of the pit distribution over a given material allows the distribution to be transposed accurately in the case of similar flow [4]. Nevertheless it may be preferable to establish a hydrodynamic intrinsic criterion of the cavitation erosion intensity of a given cavity development, and develop methods to measure this intensity, in order to decide during the tests if this cavity length is acceptable. The aim of this paper is to propose a hydrodynamic definition of the cavitation erosion intensity based on :

- an identification of the type of erosive cavitation;
- a model of the generation of transient cavities corresponding to that type of cavitation;
- the dynamic process leading to transient cavity collapse and to material damage.

The concept of this cavitation erosion intensity, defined as the mean potential power of the transient cavities, is validated with erosion experimental results obtained with electrochemical erosion detectors, and a possible measuring method is examined through vibratory level measurement.

IDENTIFICATION OF THE EROSIVE CAVITIES

As far as severe erosion of hydraulic machines is concerned we may consider, except maybe for the particular case of Pelton turbines, a corresponding development of a leading edge cavity on the blades of the runner. Systematic comparisons between visualizations carried out during model tests, and observations of damage on the prototype during periodic field visits, allow us to identify erosive cavities as swirling transient cavities shed away in the closure region of the main leading edge cavity [5]. In this region of the flow, where pressure recovery takes place, the transient cavities are subject to collapse, leading to blade erosion.

We can examine, for instance, the following example taken from [5] concerning a Francis turbine with a specific speed of $n_q = 66$ ($\nu = 0.42$). The prototype unit with a nominal power of 190 MW operated under a nominal head of 80 m. A first inspection, after 5,000 hours of operation, led to a repair, by welding with Stellite 21, of the area limited by the white contour in the photograph of the prototype runner inlet edge shown in Figure 5. This part of the runner was made of 308 stainless steel as a preventive measure. The photograph in Figure 5 was taken during a second inspection after 17,000 hours of operation, 12,000 hours after the previous field repair. The coat of paint was removed from every blade in the area of the fillet between the inlet edge of the suction side and the shroud. Pitting was observed on the region limited by the black contour; maximum erosion took place at 18 % of the chord, just upstream of the Stellite layer, which was only roughened.

If we consider the cavitation tests on the model at the contractual loads 90%, 95% and 100% respectively, for a nominal head coefficient 2% higher than that of the best operating point, the observations reveal an inlet cavitation development in the region which corresponds closely to the region of the damage. This inlet cavitation has the same pattern in all three cases; a full three-dimensional cavity attached to the blade leading edge followed, by transient cavities for which the swirling motion is well marked, as shown in the photograph in Figure 6, taken for the plant cavitation number and corresponding to the full load operation. According to the theoretical inlet flow vector diagrams corresponding to the previous three operating points, the formation of the cavity is due to high incidence flow, as in the case of the centrifugal pump presented in the introduction. The strong swirling motion of the transient cavities seems to be produced by the shearing of the flow in this part of the runner, as will be seen in the next section. However, it appears certain that the damaged areas on the blades extend in the wake of the fixed cavity. In the region of the cavity closure, unsteady vortex cavity structures are created and convected downstream to the pressure recovery region of the flow field. In these regions, the repeated vortex cavity collapses lead to damage of the blade wall material, resulting in severe erosion of the blade surface.

Fig. 5 Cavitation damages close to the shroud on the suction side of the runner inlet edge of the prototype runner of an $n_q = 66$ Francis turbine after 17,000 hours of operation; nominal head Hn = 80 m; nominal power 190 MW.

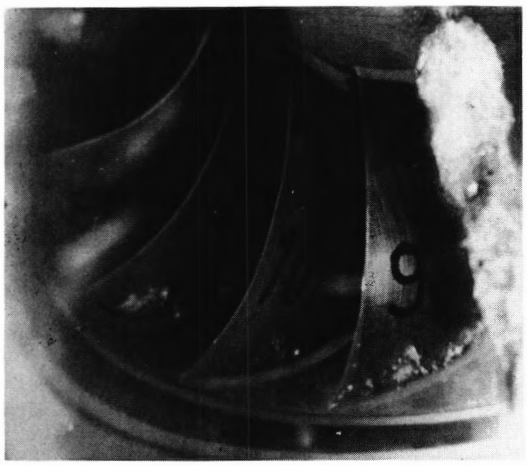

Fig. 6 Cavitation test at the plant cavitation number; the operating point corresponds to the full load and the nominal head $Q/Q_\Lambda = 1.13$.

TRANSIENT CAVITY GENERATION PROCESS

A flow survey of leading edge cavitation in the case of a 2-D hydraulic profile was carried out at high Reynolds numbers $2\ 10^6$ to $4\ 10^6$, in the IMHEF High-Speed Cavitation Tunnel [6]. Both high-speed visualization and Laser Doppler Anemometry show that the transient swirling cavities which collapse in the closure region of the main leading edge cavity originate from flow instabilities at the detachment of the main cavity at the leading edge. This detachment occurs through a spanwise distribution of cavitating spots which develop downstream to form cavitating cones. These cone-shaped cavities interact with the spanwise vortices, situated at the edge of the stationary cavity, and deform these vortices into intense Λ-shaped cavitating vortices. The mean trajectory of these discrete structures shed from the cavity detachment can be observed on the streamlines computed from the LDA mean data, Figure 7. The vertical deviation of their trajectories corresponds to the rapid growth of the flow instability and the ejection of vortices up to the outer flow, according to the sketch in Figure 8.

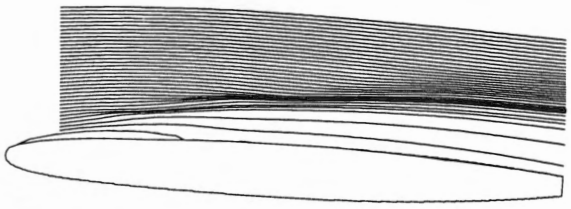

Fig. 7 Mean streamlines integrated from the LDA data in the case of leading edge cavitation $\sigma = 0.81$ and flow incidence = 2.5.

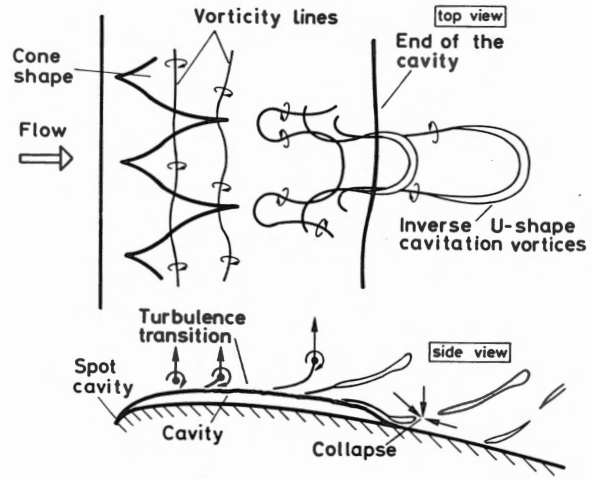

Fig. 8 Sketch of the generation process of transient swirling cavities in the case of leading edge cavitation.

Power density spectra obtained from frequency analysis of the fluctuating velocities in the closure region of the leading edge cavity allow the transient cavity shedding modulated by the fluctuation of the leading edge cavity to be observed. Bursts of swirling cavities are shed away with the mean cavity fluctuation frequency which follows a constant Strouhal number law based on the mean cavity length and the upstream velocity.

$$S = \frac{f \cdot l}{U_\infty} \qquad [-]$$

These measurements lead to the following value of the Strouhal number averaged from the data in Table 1.

$$S = 0.28 \pm 0.02 \qquad [-]$$

U_∞	l	f	S
20.70 m/s	0.032 m	179 Hz	0.277
30.00 m/s	0.042 m	191 Hz	0.268
35.00 m/s	0.048 m	225 Hz	0.309

Table 1 Length, fluctuation frequency and corresponding Strouhal number of the leading edge cavity as a function of the upstream velocity $\sigma = 0.81$ and incidence = 2.5.

This is further confirmed by systematic measurement of vibratory levels generated by this type of cavitation on the same profile, for a wide range of cavitation numbers and flow incidences [7]. According to Figure 9, the modulation frequency follows a linear relationship with the ratio U_∞/l leading to a mean Strouhal number of 0.30. In any case, these values are very close to those obtained by Kubota et al. [8] using conditional sampling techniques.

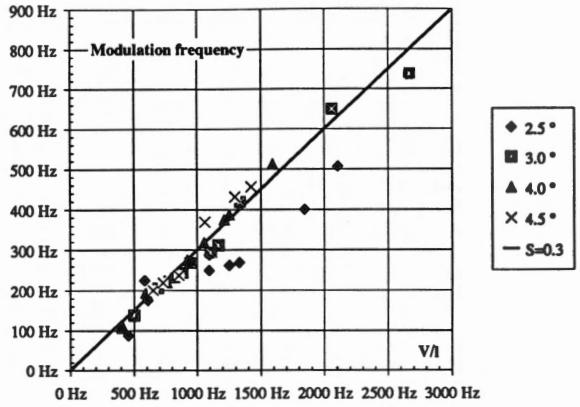

Fig. 9 Modulation frequency of the vibratory level produced by the fluctuation of a leading edge cavity as a function of the U_∞/l ratio.

DYNAMICS OF THE TRANSIENT CAVITY

If a direct study of the mechanisms involved in the collapse of the swirling vapor structures in the closure region of a leading edge cavity were the most straightforward one, it appears practically impossible to measure directly the pressure generated by the collapse. For this reason, the dynamics of this type of cavity is investigated in a special vortex generator which is able to produce a cyclic growth and collapse of a single cavitation vortex. High-speed visualization allows the formation of very intense shock wave emitted at the time of the cavity collapse and moreover to compute the shock overpressure value to be followed see [9]. By varying the operating parameters of the cavitation vortex generator it is then possible to investigate the influence of the flow rate and the cavitation number on the shock overpressure. Assuming that the total energy of the cavitation vortex is given by the potential energy of the cavity corresponding to its maximum size, we can introduce, to scale the shock overpressure, the following potential energy E

$$E = (p_{wall} - p_v) \cdot V \qquad [J]$$

where V is the maximum cavity volume, p_v is the vapor pressure and p_{wall} is the pressure at the wall of the test section in steady conditions. The difference ($p_{wall} - p_v$) represents the value of the back pressure which forces the cavity to collapse. According to our system of reference variables, the potential energy takes the form :

$$E = (C_{pwall} + \sigma) \cdot \frac{1}{2} \rho U^2 \cdot V \qquad [J]$$

Considering that the volume V is less influenced by the operating parameters we can assume that the vapor fills the entire volume of the test section during the expansion stage. This leads to the energy evaluations in Figure 10, where a monotonic increase of the mean values of the shock overpressure with the potential energy E can be observed.

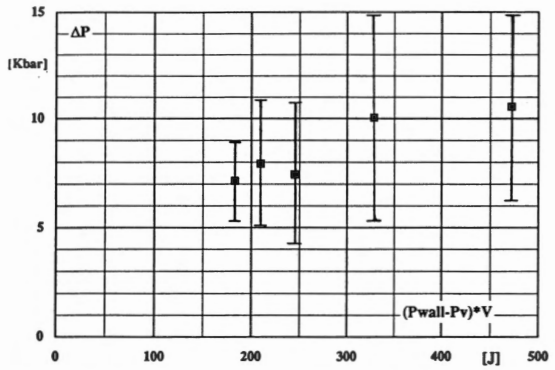

Fig. 10 Shock overpressure of the cavity collapse in the Cavitation Vortex Generator as a function of the cavity potential energy E.

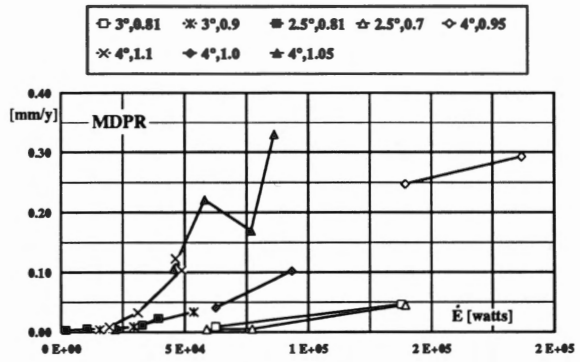

Fig. 11. Mean Depth Penetration Rate as a function of the mean cavitation erosion power term.

CAVITATION EROSION POWER

Since this potential energy term appears to be the proper scaling parameter of the collapse overpressure of a single swirling cavity, it is important to check if this term remains valid in representing the cavitation erosion intensity of a leading edge cavitation development. Thus, the corresponding term is evaluated in the case of the NACA 009 stainless steel profile equipped with 7 DECER electrochemical cavitation erosion detectors, see [10], in order to obtain simultaneous monitoring of the actual erosion rate. The growing process of a swirling cavity over the main leading edge cavity leads to a volume V of vapor which experiences, in the closure region, a back pressure p_{max} forcing the cavity to collapse. Then, the potential energy E of a single cavity collapse can be estimated as :

$$E = (p_{max} - p_v)\, V \qquad [J]$$

By introducing the cavity shedding frequency f, the mean erosive power of all the swirling cavities is:

$$\dot{E} = (p_{max} - p_v)\, V\, f \qquad [W]$$

Even though the volume of the swirling cavities V is not directly measured, a characteristic volume can be built up by assuming that the main cavity length l is the characteristic geometrical length scale of the swirling cavity generation and collapse process. It follows that the cavity volume is scaled by a cubic power of l.

Moreover according to the shedding process of the cavities, the mean shedding rate is strongly modulated by the pulsation frequency of the main leading edge cavity, which is driven by a constant Strouhal number law. Thus, the mean erosive power can be estimated by the following equation :

$$\dot{E} = \tfrac{1}{2}\rho F(Cp_{max} + \sigma)\, U_\infty^{2.]3} S \frac{U_\infty}{l} \qquad [W]$$

where the function $F(Cp_{max} + \sigma)$ is introduced to condense in one term the influence of the cavitation number σ and of the flow incidence. This equation becomes :

$$\dot{E} = \tfrac{1}{2}\rho F(Cp_{max} + \sigma)\, S\, U_\infty^{3.]2} \qquad [W]$$

From the expression of the mean cavitation erosion power, we could evaluate this term from the data of the experiments described in [4] and [7]. The corresponding mean depth penetration rates are given in Figure 11 as a function of the mean cavitation erosion power scaling term, assuming that F = 1.

The linear trend between these values and the erosive mean power for a given set of incidence and σ values leads us to plot the slope of these lines, expressed in Newton units as a function of the σ cavitation number, Figure 12. It is important to note that, even for linear plot axes, the data tend to collapse to one curve above a given threshold. The decrease in the slope at lower σ can be seen as a decrease in the erosive efficiency of the cavities, as many cavity implosions do not impact the profile in the case of a more developed leading edge cavity. The other remarkable aspect is the existence of a threshold corresponding to the limit of the actual material resistance to the erosion. However, these results allow, in any case, this mean power term to be considered as a significant term for scaling the potential erosiveness of a given cavity development.

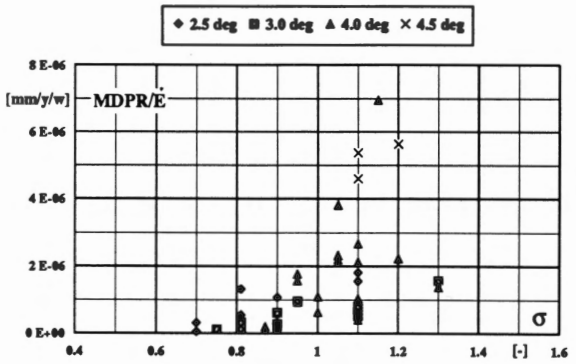

Fig. 12. Ratio of the Mean Depth Penetration Rate and the mean cavitation erosion power term as a function of the cavitation number σ.

VIBRATORY MEASUREMENT OF THE CAVITATION EROSION POWER

The direct measurement of this cavitation erosion power is difficult in the case of cavitation model test of the hydraulic machine. For a low head operating point cavity development takes place on the "pressure sides" of the blades and it is impossible to determine accurately the cavity length . Consequently, it appears to be interesting to measure indirect quantities such as vibration levels [11] or hydrodynamic noise[12] and to relate these quantities to the cavitation erosion power.

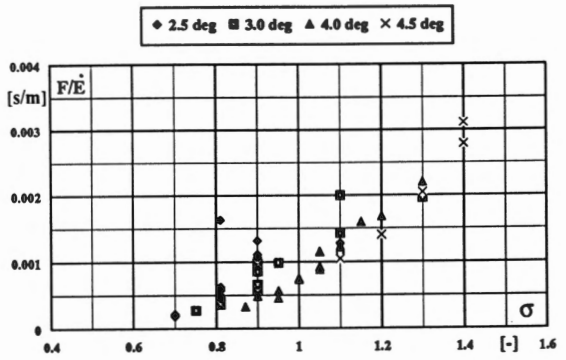

Fig. 13. Ratio of the RMS values of transient forces acting on the profile in the 15 kHz - 30 kHz range with the mean cavitation erosion power term as a function of the cavitation number σ.

In the case of the NACA 009 profile installed in the IMHEF High-Speed Cavitation Tunnel, high-frequency vibration sensors allow forces acting on the profile from a measured transmissibility function to be inferred and then the corresponding values to be related to both the mean depth penetration rate and the cavitation erosion power term, see [7]. The ability of the vibratory method to detect cavitation erosion is verified by finding, above a low threshold value, a linear relationship between the measured mean square value of the forces and the average mean depth penetration rate. However, it is possible to relate these forces to the erosion power leading to Figure 13 where, similar to Figure 12, the ratio of the RMS value of the transient forces in the frequency range of 15 kHz - 30 kHz with the scaling term of erosion power is reported as a function of the cavitation number σ. The same trend in collapsing the data in one curve is observed. Any threshold is observed since any material property is taken into account.

CONCLUSION

With a view to obtaining a proper setting of hydraulic machines, the use of a cavitation erosion power term to measure cavitation "intensity" seems to be very interesting. This hydrodynamic term, independent of any material property, is based on the model of the generation process of transient cavities in the case of leading edge cavitation. The scaling term of this cavitation erosive power depends on the upstream velocity, the cavity length and the Strouhal number of the main cavity fluctuation according to the following expression :

$$\boxed{\tfrac{1}{2}\rho S U_{\infty}^{3.12}} \qquad [W]$$

By using this scaling term it is then possible to collapse in one curve the data of the erosion experiment, which allows this curve to be transposed to the case of the prototype unit. Moreover, a relevant indirect method, such as measurement of vibratory levels, can be very useful during the current practice of cavitation tests in order to detect the cavitation erosion risk. However, if this definition of cavitation intensity appears to be valid, it is necessary to confirm its usefulness by performing more tests in the case of a model of a hydraulic machine installed on the IMHEF test rig.

ACKNOWLEDGEMENT

The authors are particularly grateful to Raynald Simoneau and Paul Bourdon from Hydro-Québec, who performed the electrochemical and vibration measurements. These experiments would not have been possible without the help of the members of the IMHEF Cavitation Research Group. This research is financially supported by the Swiss Federal "Commission d' Encouragement à la Recherche Scientifique", the Swiss Energy Producers Association "Nationaler Energie Forschung Fonds", Sulzer Brothers and Hydro Vevey .

REFERENCES

[1] Henry, P., "Hydraulic machine model acceptance tests", *Proc. of an International Conference on Hydropower Plant*, Water Power '85, Las Vegas, 1985, vol 2, pp. 1258-1267.

[2] Thiruvengadam, A., "Scaling laws for cavitation erosion." *Proc. of IUTAM Symposium on Flow of Water at High Speeds*, Leningrad (USSR), June, 1971, pp. 405-425.

[3] Kato, H, Maeda, M., Nakashima, Y.,"A comparison and evaluation of various cavitation erosion test methods", *Proc. of Symposium on Cavitation Erosion in Fluid Systems, ASME,* Boulder (Colorado), 22-24 June, 1981, pp. 83-94. .

[4] Lecoffre, Y., Marcoz, J., Franc, J. P., and Michel, J. M. "Tentative Procedure for Scaling Cavitation Damage" *Proc. of Symposium on Cavitation in Hydraulic Structures and Turbomachinery, ASME,* Albuquerque (New Mexico), 24-26 June., 1985, FED Vol.25, pp. 1-11.

[5] Avellan, F., and Dupont, Ph., "Cavitation erosion of hydraulic machines: generation and dynamics of erosive cavities." *Proc. of 14th I.A.R.H. Symposium on Progress within Large and High Specific Energy Units*, Trondheim (Norway), 20-23 June, 1988, pp 725-738.

[6] Avellan, F., Dupont, Ph., Ryhming, I.L., "Generation mechanism and dynamics of cavitation vortices downstream of a fixed leading edge cavity", *Proc. of 17th Symposium on Naval Hydrodynamics*, The Hague (The Netherlands), August 29- September 2, 1988, Sessions V, pp. 1 - 13.

[7] Bourdon, P., Simoneau, R., Avellan, F., Farhat, M., "Vibratory characteristics of erosive cavitation vortices downstream of a fixed leading edge cavity", *Proc. 15th IARH Symposium* , Belgrade (Yugoslavia), 11-14 September 1990, paper H3, pp. 1-12.

[8] Kubota, S., Kato, H., Yamaguchi, H., and Maeda, M., "Unsteady Structure Measurement of Cloud Cavitation on a Foil Section Using Conditional Sampling Technique", *Proc. of International Symposium on Cavitation Research Facilities and Technics, ASME Winter Annual Meeting,* Boston (USA), 13-18 Dec., 1987, FED-Vol. 57, pp. 161-168.

[9] Avellan, F., Farhat, M., "Shock pressure generated by cavitation vortex collapse", *Proc. of International Symposium on Cavitation Noise and Erosion in Fluid Systems, ASME Winter Annual Meeting*, San Francisco (USA), Dec 1989, FED-Vol. 88, pp 119-125.

[10] Simoneau, R., Avellan, F., Kuhn de Chizelle, Y., "On line measurement of cavitation erosion rate on a 2D NACA profile", *Proc. of International Symposium on Cavitation Noise and Erosion in Fluid Systems, ASME Winter Annual Meeting*, San Francisco (USA), FED-Vol. 88, Dec 1989, pp 95-102.

[11] Bourdon, P., Simoneau, R., Lavigne, P., "A vibratory approach to the detection of erosive cavitation", *Proc. of International Symposium on Cavitation Noise and Erosion in Fluid Systems, ASME Winter Annual Meeting*, San Francisco (USA), FED: Vol. 88, Dec 1989, pp 95-102.

[12] Abbot, P.A., "Cavitation detection measurements on Francis and Kaplan Hydroturbines", *Proc. of International Symposium on Cavitation Noise and Erosion in Fluid Systems, ASME Winter Annual Meeting*, San Francisco (USA), FED: Vol. 88, Dec 1989, pp 103-109.